DNA-Dependent Conformational Changes in the Ku Heterodimer[†]

Jason A. Lehman,*[,‡] Derek J. Hoelz,[§] and John J. Turchi[§,||]

Biomedical Sciences Graduate Program, Wright State University, Dayton, Ohio 45435, and Department of Medicine and Department of Biochemistry and Molecular Biology, Indiana University School of Medicine, Indianapolis, Indiana 46202

Received November 16, 2007; Revised Manuscript Received January 24, 2008

ABSTRACT: Ionizing radiation induces DNA double-strand breaks which are repaired by the nonhomologous end joining (NHEJ) pathway. NHEJ is initiated upon Ku binding to the DNA ends and facilitating an interaction with the DNA-dependent protein kinase catalytic subunit (DNA-PKcs). This heterotrimeric DNA-PK complex is then active as a serine/threonine protein kinase. The molecular mechanisms involved in DNA-PK activation are unknown. Considering the crucial role of Ku in this process, we therefore determined the influence of DNA binding on the structure of the Ku heterodimer. Chemical modification with NHS-biotin and mass spectrometry were used to identify sites of modification. Biotinylation of free Ku revealed several reactive lysines on Ku70 and Ku80 which were reduced or eliminated upon DNA binding. Interestingly, in the predicted C-terminal SAP domain of Ku70, biotinylation patterns were observed which suggest a structural change in this region of the protein induced by DNA binding. Limited proteolytic digests of free and DNA-bound Ku revealed a series of unique peptides, again, indicative of a change in the accessibility of the Ku70 and Ku80 C-terminal domains. A 10 kDa peptide was also identified which was preferentially generated under non-DNA-bound conditions and mapped to the C-terminus of Ku70. These results indicate a DNA-dependent movement or structural change in the C-terminal domains of Ku70 and Ku80 that may contribute to DNA-PKcs binding and activation. These results represent the first demonstration of DNA-induced changes in Ku structure and provide a framework for analysis of DNA-PKcs and the mechanism of DNA-PK activation.

The nonhomologous end joining (NHEJ)[1] pathway resolves DNA double-strand breaks (DSBs) induced by exogenous sources, including ionizing radiation (IR), and endogenous sources such as V(D)J recombination. Repair of these breaks by NHEJ is critical as DSBs pose a severe threat to genomic stability (*1*). NHEJ like other DNA repair pathways utilizes multiprotein complexes that repair DNA damage through protein−DNA and protein–protein interactions. The initial recognition step of NHEJ is carried out by the Ku heterodimer binding to the DNA termini of the DSB, followed by binding of the 469 kDa DNA-dependent protein kinase catalytic subunit (DNA-PKcs). The formation of the heterotrimeric DNA-dependent protein kinase (DNA-PK) results in autophosphorylation of serine/threonine residues in DNA-PKcs. Both Ku and DNA-PKcs represent essential components of double-strand break repair. Genetic and biochemical evidence has determined that the DNA ligase IV−XRCC4 (L4−X4) complex is a mammalian DNA ligase that is responsible for resolving the ends during NHEJ (*2*). Ku has been shown to facilitate binding of the L4−X4 complex to DNA ends and increase the ligation efficiency (*3*). DNA end processing is accomplished by the Artemis endo/exonuclease (*4, 5*), while the X-family polymerases also participate in end processing via nucleotide addition (*6*). In addition, the XLF/Cernunnos protein was recently identified and has been shown to interact with and stimulate the DNA ligase IV−XRCC4 complex (*7–9*).

The Ku molecule is a heterodimer composed of 70 and 80 kDa subunits. Ku binds broken DNA ends with an extremely high affinity in a manner independent of a sequence context. A duplex DNA substrate with a minimal length of 14 bases has been determined to facilitate a binding event of one Ku molecule (*10*). Ku was crystallized in a manner such that one Ku molecule was bound per DNA molecule. Ku forms a unique structure where it has a hollow preformed channel in the absence of DNA termed the bridge and pillar region, and this is where DNA binding and threading occur. Data from the crystal structure reveal that the Ku heterodimer utilizes primarily positively charged and hydrophobic amino acid contacts on both Ku70 and Ku80 polypeptides for DNA binding. These form contacts with the sugar–phosphate backbone rather than the DNA bases themselves (*11*). The directional orientation of the heterodimer positions the von Willebrand A (vWA) homology α/β domain of the Ku70 subunit toward the end of the DNA break, while the vWA α/β domain of Ku80 comes in contact

[†] This work was supported by NIH Grant CA82741 (J.J.T.) with additional support from the Walther Cancer Institute.

* To whom correspondence should be addressed: Indiana University Cancer Research Institute, R4-202, 1044 W. Walnut St., Indianapolis, IN 46202. Telephone: (317) 278-1996. Fax: (317) 274-0396. E-mail: jturchi@iupui.edu.

[‡] Wright State University.

[§] Department of Medicine, Indiana University School of Medicine.

[||] Department of Biochemistry and Molecular Biology, Indiana University School of Medicine.

[1] Abbreviations: DSB, DNA double-strand break; NHEJ, nonhomologous end joining; DNA-PK, DNA-dependent protein kinase; DNA-PKcs, DNA-PK catalytic subunit; CTD, C-terminal domain; NHS-biotin, *N*-hydroxysuccinimidobiotin; LC-Q, liquid chromatography ion trap quadrupole; MS, mass spectrometry; ESI, electrospray ionization; vWA, von Willebrand A; SAP, SAF-A/B Acinus and PIAS.

10.1021/bi702284c CCC: $40.75
Published on Web 03/21/2008

with the dumbbell-shaped end of the substrate used for crystallization.

Much of the structural analysis of Ku has been accomplished with truncated forms of the heterodimer. The final crystal structure of non-DNA-bound Ku contained 60% of the amino acids, while the DNA-bound Ku cocrystal contained 53% of the total amino acids. This includes the absence of the Ku70 C-terminal domain (CTD) from the non-DNA-bound Ku structure and the Ku80 CTD which was enzymatically cleaved by trypsin prior to crystallization. A separate NMR solution structure of the Ku70 C-terminal domain has revealed it is comprised of a flexible linker region that ends in a three-α-helix motif, both capable of binding DNA (*12*). The structure of the Ku80 CTD has warranted enough interest to produce two separate NMR studies yielding a structure containing six α-helices with multiple loops, with one loop that forms a disordered tail to which the DNA-PKcs is presumed to bind (*13, 14*). The binding event of DNA-PKcs is known to involve at least residues 720–732 of Ku80 (*15*). However, because of the large size of DNA-PKcs, it is more likely that additional contacts are made between the surfaces of Ku and remain to be elucidated. Thus, complete information about how DNA binding changes the entire structure of Ku is lacking and could improve our understanding of the damage recognition step in NHEJ.

In this study, we have examined the consequence of DNA binding for the complete structure of Ku in solution. A series of determined novel changes have been observed using limited proteolysis, chemical modification, and mass spectrometry. Limited proteolysis of free and DNA-bound Ku followed by probing with site-specific antibodies revealed DNA-dependent changes in the accessibility of the C-terminus of Ku70 and Ku80. These are likely manifested by movement or conformational changes in these domains and their proximity to other domains within Ku and the DNA substrate. Chemical modification of lysine residues with NHS-biotin identified novel sites in the C-terminus of Ku70 that were differentially biotinylated in the absence of DNA versus DNA-bound conditions, while no detectable changes in the C-terminus of Ku80 were observed. A small 10 kDa peptide that was generated only under non-DNA-bound conditions was also found to map to the C-terminal region of Ku70. These data suggest that both the Ku70 and Ku80 C-termini undergo structural remodeling upon binding duplex DNA and provide further insight into individual steps for recognition of DNA double-strand breaks in the NHEJ pathway.

EXPERIMENTAL PROCEDURES

Materials. The following materials were purchased from the indicated sources. Modified sequencing-grade trypsin was purchased from Roche and [γ-^{32}P]ATP (3000 Ci/mmol) from Perkin-Elmer. L-Lysine, tricine, and iodoacetamide were from Sigma. *N*-Hydroxysuccinimidobiotin was from Pierce. Mouse monoclonal antibodies against Ku70 Ab-4 (N3H10) and Ku80 Ab-2 (111) were from Neomarkers. Goat polyclonal antibodies against Ku70 (C-19) were from Santa Cruz Biotechnology. DNA oligonucleotide substrates were purchased from Integrated DNA Technologies.

DNA Substrates and Proteins. The following DNA substrates were used: 21-mer, 5′-GTTTTTAGTTTATTGGGCGCG-3′; 31-mer, 5′-GGGATACTCCGTTGCTAGTTTATTGGGCGC-G-3′; 34-mer, 5′-CGCGCCCAGCTTTCCCAGCTAATAAACTAAAA-AC-3′; and 44-mer, 5′-CGCGCCCAGCTTTCCCAGCTAATAA-ACTAGCAACGGAGTATCCC-3′. The 21-mer−34-mer duplex was the substrate used for Ku crystallization, while the 31-mer and 44-mer substrates represent analogous substrates with 10-base extensions on each (*11*). The 21-mer substrate was annealed to its complement 34-mer at a 3:1 molar ratio and annealed duplex viewed on a preparative 12% native polyacrylamide gel to ensure minimal unannealed single-stranded DNA was present. The human Ku heterodimer was overexpressed from recombinant baculovirus in insect cells as previously described (*16*). Ku was purified in a one-step purification process using a Ni-NTA column, dialyzed in 50 mM HEPES (pH 8.0), 50 mM NaCl, and 2 mM DTT in the absence of protease inhibitors, and stored at −80 °C. SDS−PAGE and Coomassie staining showed Ku to be 95% pure from other contaminating proteins.

EMSAs. EMSAs were performed as previously described (*17*) with some minor modifications. Briefly, reactions were performed in a buffer containing 50 mM Tris-HCl (pH 7.8) and 50 mM NaCl in a reaction volume of 20 μL. Reaction mixtures contained 100 fmol of ^{32}P-labeled 21-mer−34-mer duplex DNA with a titration of Ku as indicated in the figure legends. After amino acid chemical modification, Ku was dialyzed again in the purification dialysis buffer to remove any unwanted reaction contaminants prior to the EMSA. Reactions were carried out for 10 min on ice and the mixtures loaded onto 6% native polyacrylamide gels and run with cold 1× TBE buffer. Gels were dried and exposed to a PhosphorImager screen and quantified using ImageQuant (GE Healthcare Life Sciences).

Tris−Tricine Gel Electrophoresis. Tris−Tricine gels (16%) were prepared according to a previously published procedure for separation of peptides (*18*). Gels were electrophoresed for 3.5 h at a constant power of 6 W with a cooling water jacket. Protein bands were visualized with Coomassie blue G-250 and silver staining as indicated.

Biotin Modification and In-Gel Tryptic Digestion. Amino acid chemical modification of lysine residues was done with *N*-hydroxysuccinimidobiotin (NHS-biotin). Purified Ku was modified in the presence and absence of the duplex 21-mer−34-mer oligonucleotide. Ku (0.5 μM) was preincubated with or without the addition of 2 μM DNA substrate in a protein modification buffer containing 50 mM HEPES (pH 7.5), 50 mM NaCl, and 2 mM DTT in a reaction volume of 100 μL. DNA binding reaction mixtures were incubated for 10 min at room temperature. Biotin modification was performed at final concentrations of 100 or 400 μM NHS-biotin or mock-treated with an equivalent volume of DMSO for controls. Modification reactions were performed for 25 min at room temperature and stopped with the addition of 10 mM lysine followed by separation of the 70 and 80 kDa subunits of Ku by 10% SDS−PAGE. The gel was then stained with Coomassie blue and destained in 10% acetic acid and 5% methanol. Ku70 and Ku80 protein bands were excised from the gel and dehydrated with 25 mM NH_4CO_3 and 50% acetonitrile and treated with 10 mM DTT in 25 mM NH_4CO_3 at 55 °C for 45 min, followed by a treatment with 55 mM iodoacetamide at room temperature for 30 min.

Gel pieces were then washed with 25 mM NH_4CO_3 and dehydrated with 25 mM NH_4CO_3 and 50% acetonitrile, followed by addition of 440 ng of bovine trypsin in 25 mM NH_4CO_3 at a concentration of 12.5 ng/μL. Samples were digested with trypsin overnight at 37 °C. A 50% acetonitrile/5% formic acid solution was added the following day with shaking and sonication to release peptides. Samples were dried under vacuum, and 10 μL of 1% formic acid was added prior to LC−MS/MS analysis.

Limited Proteolysis. Ku (8–16 μg) was analyzed in reaction mixtures containing 50 mM HEPES (pH 8.0), 50 mM NaCl, and 2 mM DTT. DNA was added to reaction mixtures in excess like in the biotin modification procedure. The reaction mixtures were incubated on ice for 10 min prior to the addition of trypsin as indicated in the figure legends and then incubated at 37 °C for 45 min. The reactions were stopped when the samples were heated to 90 °C for 5 min and loaded onto either a 15% SDS−polyacrylamide gel or a 16% Tris−Tricine polyacrylamide gel. Protein was detected with either Coomassie blue G-250 or silver stain as indicated.

Mass Spectrometry. Ku (8–16 μg) was subjected to limited proteolysis as indicated above. Exhaustive digests from biotinylation reactions or bands identified on Coomassie- or silver-stained gels were subjected to in-gel tryptic digestion as indicated above. Digested samples were then resuspended in 1% formic acid prior to being assessed by LC−MS/MS. Data were obtained using a Surveyor MS pump and an AS3000 autosampler and a LC-Q Advantage ion trap tandem mass spectrometer (Thermo-Fisher Corp.) fitted with a custom-made nanospray source (*19*). Peptides were separated via reverse phase high-performance liquid chromatography using a 0.1 mm × 30 mm, 5 μm, 200 Å, C-8 (Michrom Bioresources, Inc.) trap column and a 0.05 mm × 150 mm, 5 μm, 100 Å, Magic C-8 analytical column/nanospray emitter packed in house. The column was equilibrated, and samples were loaded on the column in buffer A (0.1% formic acid) at a rate of 4 μL/min. Peptides were eluted with a linear gradient from 2 to 50% buffer B (0.1% formic acid in acetonitrile) over 80 min at a rate of 0.15 μL/min. Raw MS/MS data were searched using the MASCOT (www.matrixscience.com) search engine, and an error tolerant search was performed to identify peptides with carbamidomethylations of cysteines, oxidized methionines, and biotinylation of lysines as modifications to peptides. Positive hits for peptides containing possible biotinylated lysines were then subjected to further identification by visual interpretation of the raw MS/MS data. Biotinylated peptides showed an increase in mass of 226.4 Da on a lysine residue. Qualitatively, data were examined to determine if protection from biotin occurred in peptides in which Ku was prebound to DNA compared to their biotinylated (or nonbiotinylated) counterpart in samples in which Ku was not prebound to DNA. This differentially identified which lysine residues had changes in solvent accessibility and contact with DNA. Under conditions where Ku was preincubated with DNA, the identification of the nonbiotinylated peptides or peptide fragments was performed to ensure that a nonbiotinylation event was not due to a sequence coverage loss of that particular sequence.

RESULTS

Changes in Ku Accessibility upon DNA−Ligand Binding. To elucidate the effect of DNA binding on the full-length Ku heterodimer and possibly detect unique movement of specific domains or formation of secondary structural regions in the protein, we initially examined the Ku−DNA interaction by limited proteolysis. Purified Ku was incubated in the absence or presence of DNA and then subjected to digestion with trypsin. The trypsin digestion conditions were designed to minimize dissociation of Ku from the DNA, and according to our previous results, less than 10% dissociation occurs during the trypsin reaction (*17*). Analysis of a range of trypsin concentrations revealed trends in peptides generated under DNA-bound Ku or Ku alone conditions. The results presented in Figure 1 show a significantly greater degree of generation of tryptic peptides under non-DNA-bound conditions (lanes 3, 5, and 7) compared to their DNA-bound counterparts at identical concentrations of trypsin (lanes 4, 6, and 8). Control reaction mixtures (lanes 1 and 2) not treated with trypsin revealed the Ku preparation was approximately 90% pure, with the majority of the contaminants being lower-molecular mass species. The DNA substrate employed in Figure 1 is the 31-mer−44-mer duplex that contains a 24 bp duplex region that is capable of binding two Ku molecules per DNA (data not shown). Ku has been characterized as having a minimum binding requirement of 12 bp of duplex DNA. Loading of multiple Ku molecules has also been demonstrated in accordance with length of duplex DNA, where up to five molecules could be bound on a 115-mer substrate (*20*). This substrate is 10 bp longer than that of the 21-mer−34-mer substrate used for determining the structure of a Ku−DNA cocrystal (*11*). The 21-mer−34-mer and 31-mer−44-mer DNA substrates both have one end of the DNA composed of a G-rich stem and a small hairpin, which together form a dumbbell shape to prevent Ku from sliding off or displacement by another Ku molecule. To ensure that the results were not a function of multiple Ku binding events, reactions were performed in excess DNA which drives the binding equilibrium to a single Ku bound per DNA molecule. In addition, we analyzed how trypsin

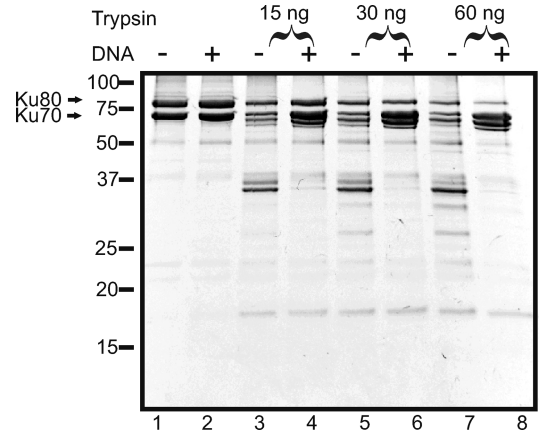

FIGURE 1: Limited proteolysis of free and DNA-bound Ku heterodimer. Eight micrograms of Ku was either left free or bound to saturating amounts of 31-mer−44-mer DNA substrate (indicated with a minus or a plus, respectively) as described in Experimental Procedures. Proteolysis by trypsin was initiated by addition of 15 ng (lanes 3 and 4), 30 ng (lanes 5 and 6), or 60 ng of trypsin (lanes 7 and 8) or no trypsin (lanes 1 and 2) and the reaction carried out for 45 min at 37 °C. Samples were run and then loaded onto a 15% SDS−PAGE gel and stained with Coomassie blue G-250 to observe peptides generated by tryptic cleavage. Positions of the undigested 70 and 80 kDa Ku subunits are indicated with arrows.

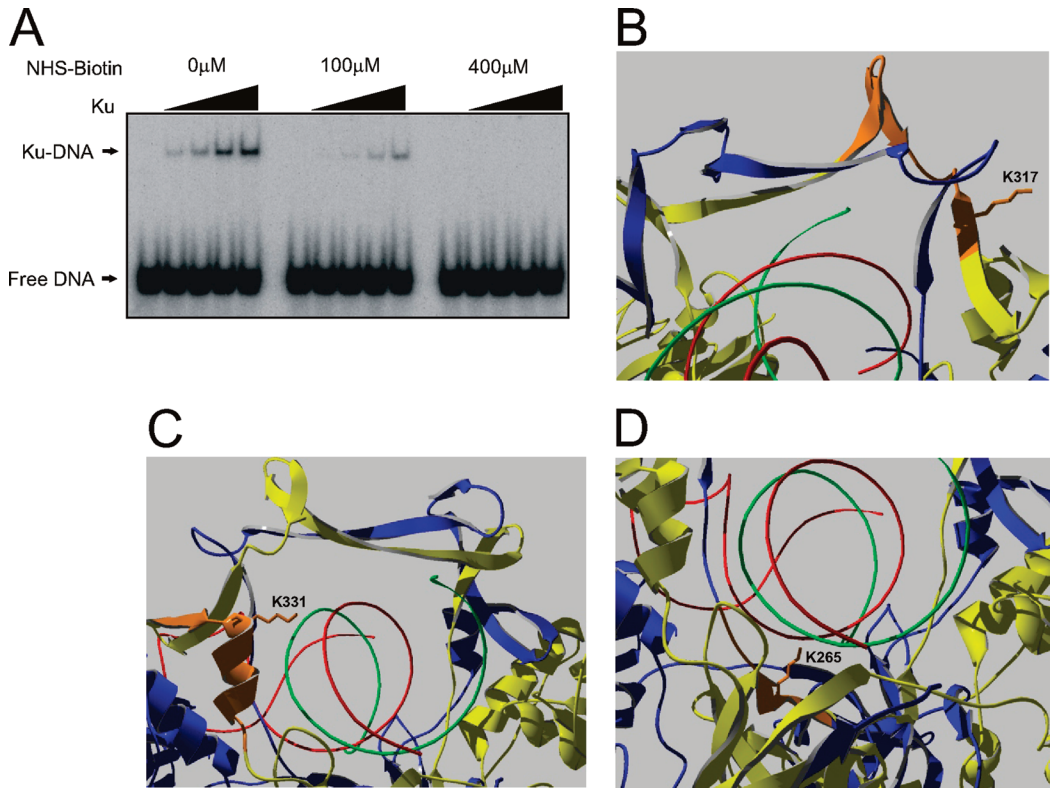

FIGURE 2: NHS-biotin modification inhibits Ku−DNA binding and protection of Ku70/Ku80-specific lysines from modification upon DNA binding. (A) An EMSA was run with purified Ku treated with 0, 100, and 400 μM NHS-biotin. Increasing concentrations of Ku were mixed with 100 fmol of a ^{32}P-labeled 21-mer−34-mer DNA substrate in lanes 2–5, while free DNA was loaded in lane 1 in all sets. (B−D) Differential biotinylation of lysine residues between free and DNA-bound Ku was analyzed by tandem mass spectrometry, and unique changes are represented in crystal structure models. (B) A peptide containing biotinylated K317 (orange) from the Ku70 subunit (yellow) detected with Ku alone and Ku−DNA complexes. (C) A peptide containing biotinylated K331 (orange) from the Ku70 subunit (yellow) was found only under non-DNA-bound conditions. The 21-mer−34-mer DNA is depicted in red and green with the Ku80 subunit (blue). (D) A peptide containing K265 (orange) from the Ku80 subunit (blue) was found to be biotinylated only in the absence of DNA.

cleavage was influenced by binding to the 21-mer−34-mer substrate though Ku displays a slightly lower affinity for this substrate and the thermal stability of the DNA duplex is reduced as a function of the shorter duplex region. Importantly, we obtained nearly identical results using the two substrates, demonstrating that the Ku−Ku interactions on a single DNA were not responsible for the different cleavage patterns obtained compared to free Ku (data not shown). To ensure the results obtained were not a function of the end hairpin DNA structure, we performed a limited proteolysis experiment using a fully duplex 30-mer (*17*). Comparison of this substrate to the 21-mer−34-mer and 31-mer−44-mer duplex DNA substrates revealed no detectable differences in the pattern of peptide cleavage (data not shown). These results demonstrate that DNA binding protects regions of Ku from digestion with trypsin. This observed protection could be the result of a direct interaction with DNA such that Ku is less accessible for trypsin cleavage, DNA-induced steric hindrance causing movement of specific regions on Ku, in a way that the proteolytic pattern and efficiency of Ku are altered or a combination of both events.

Solvent Accessibility Is Altered in Ku70 and Ku80 upon DNA Binding. To further investigate the mechanism of altered trypsin cleavage and map the specific changes in Ku structure where it binds to DNA, we used covalent amino acid modification coupled with tandem mass spectrometry. This methodology provides increased resolution and the ability to pinpoint subtle changes in accessibility as a function of DNA binding. *N*-Hydroxysuccinimidobiotin (NHS-biotin) reacts specifically with lysine amino acids and results in the covalent attachment of a single biotin molecule per accessible lysine. The modification with biotin also renders the lysine resistant to tryptic digestion; thus, a postmodification trypsin digestion was employed and coupled with MS/MS to identify sites of biotin modification. We first tested the biological effect of lysine modification on Ku's DNA binding activity. Ku was treated with a range of NHS-biotin concentrations (100–400 μM), and following the reaction, unreacted NHS-biotin was quenched with excess lysine. The samples were then dialyzed to remove excess NHS-biotin lysine and reaction side products, and then DNA binding was assessed in an electrophoretic mobility shift assay (EMSA). The results presented in Figure 2A demonstrate that the following reaction with 100 μM NHS-biotin, Ku−DNA binding activity was reduced to less than 50% of control levels. Treatment of Ku with 400 μM NHS-biotin resulted in a complete abrogation of DNA binding activity. Inhibition of Ku−DNA binding can be directly attributed to modification of lysines since samples were modified, dialyzed, and then analyzed by an EMSA. In addition, mixing experiments revealed that there was no inhibitory factor in the NHS-biotin-treated Ku that could inhibit unmodified Ku after Ku was dialyzed (data not shown). Identical results were obtained with the use of the 31-mer−44-mer duplex DNA substrate (data not shown). Thus, modification of lysine residues within Ku inhibits Ku's DNA binding activity,

Table 1: MS/MS Analysis of Ku Amino Acid Chemical Modification

	peptide	Ku subunit	amino acids	biotin (K)	without DNA	with DNA
1	TFNTSTGGLLLPSDTKR	Ku70	302–318	K317	+	+
2	QIILEKEETEELKR	Ku70	326–339	K331	+	−
3[b]	ELVYPPDYNPEGKVTK	Ku70	527–542	K539	+	−
4[b]	FTVPMLKEACR	Ku70	576–586	K582	+	−
5[c]	IAAYKSILQER	Ku80	261–271	K265	+	−
6	IKTLFPLIEAKK	Ku80	533–544	K534/K543	+	+
7	FNNFLKALQEK	Ku80	655–665	K660	+	+
8	KFLAPK	Ku80	703–708	K703	+	+

[a] An in-gel tryptic digestion procedure was performed on Ku70- and Ku80-specific bands that had undergone NHS-biotin modification. Samples were run separately by LC−MS/MS to identify differences in biotinylation of lysine residues with free and DNA-bound Ku. Individual columns show the peptide sequence, corresponding amino acids, subunit identity, and individual biotinylated residues. The presence of a biotinylated lysine is indicated with a plus and a nonbiotinylated lysine with a minus in columns 6 and 7. [b] Peptides that map to regions not present in the crystal structure that display differential (K) biotinylation. [c] Residue known to make contact with phosphate in DNA and sugar from the crystal structure.

strongly suggesting that these residues are essential for Ku's DNA binding activity.

Since an effect of biotin modification was demonstrated on DNA binding, we set out to determine if DNA binding by Ku altered the reactivity of the NHS-biotin with certain lysines. For the chemical modification coupled with mass spectrometry experiments, Ku samples were bound to either 21-mer−34-mer or 31-mer−44-mer duplex DNA substrates in excess or left unbound and then treated with NHS-biotin. The reacted Ku preparations were then separated via SDS−PAGE and the Ku80 and Ku70 bands excised and subjected to exhaustive in-gel tryptic digestion. Separate samples containing either biotin-modified Ku70, Ku80, or unmodified controls were separated by reverse phase HPLC and analyzed by MS/MS. Data obtained from the LC−MS/MS experiments were searched against the Swiss-Prot protein database using the MASCOT algorithm. Upon initial identification, an error tolerant search was employed to identify peptides containing biotin and other modifications that arise from sample handling. Peptides increase in mass by 226.4 Da per biotinylated residue. A representation of biotinylated peptides from both Ku subunits and their biotinylation status as a function of DNA binding is given in Table 1. The sequences of these peptides are based on the numbering system used in the Ku crystal structure (*11*). Peptide 1 in Table 1 corresponds to amino acids 302–318 of the Ku70 subunit. The modified residue is K317 and is biotinylated in both free and DNA-bound conditions of Ku. Examination of the crystal structure of the Ku−DNA complex reveals that the R group of the lysine is on one of the pillars and is completely solvent accessible for modification by NHS-biotin as shown in Figure 2B. Peptide 2 in Table 1 has two tryptic missed cut sites in amino acids 326–339 of Ku70, where K331 represents the biotinylated lysine. K331 is also present on the pillar, and the R group of the amino acid points into the central cavity where DNA is threading through Ku (Figure 2C). K331 is always biotinylated when Ku is not bound to DNA and not modified when Ku−DNA complexes are preformed, indicating that the presence of DNA blocks chemical modification of this residue. This biotinylated lysine is within a peptide that contains another residue, K338, which was reported to make contact with a sugar in the crystal structure (*11*). Our analysis of K338 gave variable results in biotinylation status in both free and DNA-bound Ku. In the absence of DNA, K338 was always observed to be biotinylated, and upon DNA binding while we did observe nonbiotinylated peptides, the biotinylation was not completely abrogated (data not shown). This may be a result of the dynamic nature of the DNA binding process or equilibrium of bound and unbound Ku. Thus, K331 sits in the bridge−pillar region of Ku70 and is in the proximity of the duplex DNA, likely making contacts to sugar or phosphate. Two additional lysines in peptides 3 and 4 of Ku70 were found to be biotinylated only under non-DNA-bound conditions listed in Table 1. Interestingly, K539 and K582 both map to an unstructured region of Ku70 in the C-terminus from the cocrystal of the Ku−DNA complex. The K582 residue is present in the free Ku crystal structure, while K539 is still unstructured. These two amino acids likely interact with DNA and are blocked from biotinylation when Ku−DNA complexes are formed. This C-terminal region of Ku70 contains a putative SAP (SAF-A/B, Acinus, and PIAS) domain (*21*). This region is purported to contain a weak DNA-binding motif and is present in other proteins involved in DNA repair and chromosomal maintenance. Another possibility that the Ku−DNA binding event could alter the position of the domains such that the Ku70 C-terminus embeds itself in DNA that prevents biotinylation of those residues from occurring exists.

In the examination of the Ku80 subunit, a change in biotinylation was detectable in peptide 5 at K265 only under non-DNA-bound conditions shown in Figure 2D. K265 has been demonstrated from the crystal structure to make contacts with the phosphate and sugar in the DNA. This result is a good confirmation of the methodology used since this residue was previously identified to be involved in DNA binding. Since we were able to detect changes in the biotinylation status in the unstructured C-terminus of Ku70, we also examined the C-terminus of Ku80 for differential lysine modification under identical conditions. A doubly biotinylated peptide containing two lysine residues, K534 and K543, is present in the crystal structure at the start of the C-terminus of Ku80 in an α-helix and a loop. These residues are always biotinylated with both free and DNA-bound Ku due to their high solvent accessibility. Two additional peptides from amino acids 655–665 and 703–708 (peptides 7 and 8, respectively, from Table 1) are biotinylated under free and DNA-bound conditions. Two separate NMR studies have revealed that the C-terminus of Ku80 is a very open structure comprised of a series of loops and α-helices (*13, 22*). Since the solvent accessibility of the Ku80 CTD is very high, specific lysine residues were biotinylated regardless of whether free Ku or Ku−DNA complexes were formed in the reaction.

A DNA-Dependent Change in the Orientation in the C-Terminal Domain of Ku80. These alterations in biotiny-

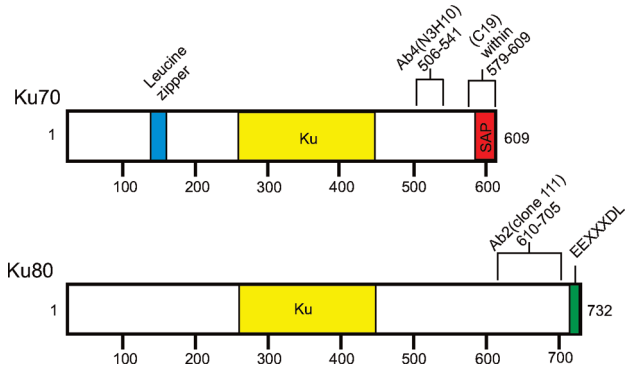

FIGURE 3: Epitope mapping of Ku70 and Ku80 domain-specific antibodies. A diagram representing the linear amino acid sequences of Ku70 (top) and Ku80 (bottom) is depicted. The Ku70 leucine zipper domain is colored blue, and the C-terminal SAP domain is colored red. The Ku80 C-terminal DNA−PKcs interaction domain is colored green, and on both subunits, the Ku domains are colored yellow. Antibodies that recognize an epitope against the C-terminus of Ku70 are diagrammed: the N3H10 antibody recognizes amino acids 506–541, and the C-19 antibody recognizes some amino acids within residues 579–609. An antibody against the C-terminus of Ku80 (Ab2 clone 111) recognizes amino acids 610–705. Numbered tick marks represent 100 amino acids for each protein.

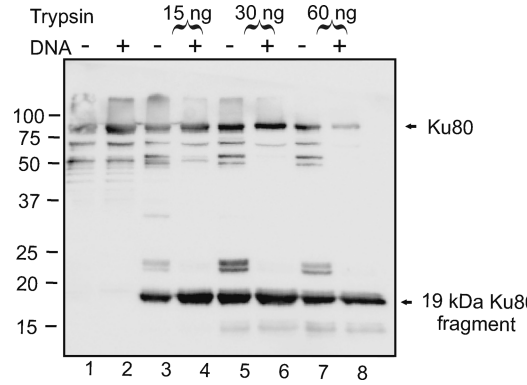

FIGURE 4: Protection of Ku80-specific peptides with Ku−DNA complexes. DNA binding reactions and proteolysis were performed in a manner identical to that described in the legend of Figure 1. Fifteen nanograms of trypsin was used in lanes 3 and 4, 30 ng in lanes 5 and 6, and 60 ng in lanes 7 and 8; no trypsin was used in lanes 1 and 2. The reaction was carried out for 45 min at 37 °C. Samples were separated on a 15% SDS−PAGE gel, transferred to a PVDF membrane, and probed with an anti-Ku80 clone 111 antibody that recognizes the C-terminus of Ku80, amino acids 610–705. Positions of undigested Ku80 and the proteolytic-sensitive 19 kDa Ku80 C-terminal region are identified with arrows.

lation patterns suggest DNA-dependent conformational changes in Ku. Therefore, we employed site-specific antibodies to examine regions of both Ku70 and Ku80 suspected to change in accessibility upon binding DNA. Once again, limited proteolysis was used to demonstrate a difference in peptides generated under free and DNA-bound conditions followed by Western blotting. These assays were employed to reveal any differences that may not be observable with amino acid chemical modification and confirm some of the differences observed with the other assay. In Figure 3 are shown functionally important domains and the particular epitopes on the proteins the antibodies recognize. An antibody against the C-terminal region of Ku80 (clone 111) (Figure 3) was able to detect the trypsin-sensitive 19 kDa Ku80 fragment (indicated with the arrow) under non-DNA-bound and DNA-bound conditions in Figure 4 (lanes 3–8), as previously reported (*11*). The antibody was able to detect some smaller products below the undigested Ku80 which could be due to the high concentration of Ku that was used per lane. These bands appear uniformly throughout the blot in lanes 1–8. In lanes 3, 5, and 7 where Ku was not reacted with DNA, the clone 111 antibody recognizes a unique doublet band which migrates above the 19 kDa C-terminal fragment between the 20 and 25 kDa protein standards compared to lanes 4, 6, and 8 of Figure 4 where the doublet is not present in Ku−DNA complexes. Since the doublet is generated by trypsin only under non-DNA-bound conditions, the possibility that DNA blocks trypsin accessibility on Ku such that these peptides are not generated exists. Another possibility is that these larger fragments are cut more frequently to generate more of the 19 kDa C-terminus and smaller fragments not observed on the 15% SDS−PAGE gel. An identical experiment was performed, and samples were separated by electrophoresis on a 16% Tris−Tricine gel to resolve peptides down to the 6 kDa range. An identical digestion pattern was observed when the blot was probed with the clone 111 antibody, and despite the increased range, no peptides below the 19 kDa C-terminal fragment were observed that could be attributed to the Ku80 CTD (data not shown). These results are consistent with the C-terminus of Ku80, represented by the doublet at 22–24 kDa, being protected from cleavage under DNA-bound conditions. These data suggest that the consequence of Ku binding to DNA initiates a DNA-dependent domain movement or remodeling of local structure in the C-terminus of the Ku80 subunit.

A DNA-Dependent Conformational Change Occurs in the Ku70 C-Terminal SAP Domain. While no Ku80 CTD peptides were observed below 19 kDa, we sought to determine if any low-molecular mass peptides were generated upon Ku digestion. Therefore, samples were separated by electrophoresis on a 16% Tris−Tricine gel, and the gel was stained with Coomassie blue. This analysis did in fact reveal the presence of peptides with molecular masses below 15 kDa (Figure 5A). A unique Ku peptide which migrated with an apparent molecular mass of 10 kDa was observed only with free Ku (lanes 3, 5, and 7). In the reaction where Ku was bound to the 21-mer−34-mer DNA, the 10 kDa band was not observed (lanes 2, 4, and 6), suggesting that DNA binding either inhibited trypsin cleavage generating the 10 kDa band or stimulated secondary cleavage within the 10 kDa peptide such that it was degraded into smaller peptides.

To determine the origin of the 10 kDa band, we carried out limited proteolysis of separated samples on Tris−Tricine gels and transferred them to a membrane to be probed with a variety of site-specific antibodies against Ku70 and Ku80. Only the Ku70 (C-19) antibody against the far C-terminal region (within the final 30 residues) reacted with the 10 kDa peptide, demonstrating that this peptide encompasses the extreme C-terminus of Ku70 (Figures 3 and 5B). The increased sensitivity of antibody detection revealed that the 10 kDa band was also generated in reactions with Ku bound to DNA and was dependent on the degree of digestion. In addition, silver staining of digests did allow detection of faint bands corresponding to the 10 kDa band (data not shown). In all experiments, at limited trypsin concentrations, the level of generation of this peptide was significantly reduced upon DNA binding. The dynamic nature of the DNA binding reactions could account for the inability to completely

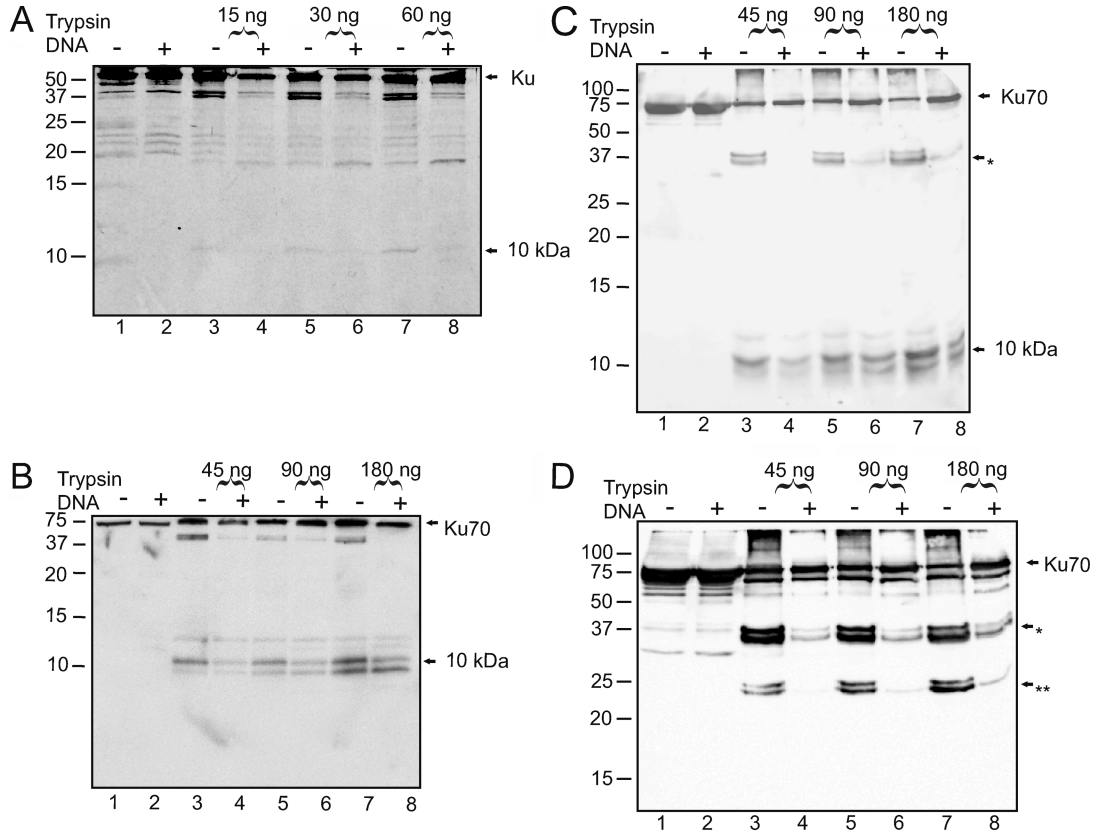

FIGURE 5: Protection of Ku70-specific peptides with Ku−DNA complexes. (A) Ku (16 μg) was either left free or bound to saturating amounts of 21-mer−34-mer DNA substrate (indicated with a minus or a plus, respectively) as described in Experimental Procedures. Limited tryptic proteolysis was initiated by addition of 15 ng (lanes 3 and 4), 30 ng (lanes 5 and 6), or 60 ng of trypsin (lanes 7 and 8) or no trypsin (lanes 1 and 2) and the reaction carried out for 45 min at 37 °C. Proteolytic Ku digests were separated on a 16% Tris−Tricine gel and stained with Coomassie blue G-250 to visualize low-molecular mass peptides. The 10 kDa peptide is indicated with an arrow. (B−D) Ku (16 μg) was either left free or bound to saturating amounts of 21-mer−34-mer DNA substrate (indicated with a minus or a plus, respectively), and proteolysis was initiated by addition of 45 ng (lanes 3 and 4), 90 ng (lanes 5 and 6), or 180 ng of trypsin (lanes 7 and 8) or no trypsin (lanes 1 and 2) with the same incubation conditions described above. (B) Samples were separated on a 16% Tris−Tricine gel, transferred to a PVDF membrane, and probed with the anti-Ku70 C-19 antibody for detection of smaller Ku70 C-terminal peptides. (C) Samples were separated on a 15% SDS−PAGE gel, transferred to a PVDF membrane, and probed with the anti-Ku70 C-19 antibody which recognizes the far C-terminal region of Ku70. (D) Samples were separated on a 15% SDS−PAGE gel, transferred to a PVDF membrane, and probed with an anti-Ku70 N3H10 antibody which recognizes the more N-terminal part of the Ku70 C-terminal portion (amino acids 506–541). The positions of the Ku70 subunit and 10 kDa peptide are indicated with arrows in Western blots. Positions of 37 kDa tryptic cleavage products are indicated with one asterisk, and the 25 kDa tryptic cleavage product is denoted with two asterisks.

abrogate the generation of the 10 kDa band or the fact that the change of blocking of trypsin accessibility is only partially reduced under these conditions.

To test if the loss of the 10 kDa band upon DNA binding was the result of using the blocked-end 21-mer−34-mer substrate, we performed an experiment using the duplex 30-mer (no blocked ends) and observed identical results where the level of generation of the 10 kDa band is reduced upon DNA binding (data not shown). While the Tris−Tricine electrophoresis (Figure 5A,B) enabled the resolution of low-molecular mass fragments, it was apparent that there were DNA-dependent differences in the generation of higher-molecular mass tryptic fragments. The analysis of similar digestions separated via traditional SDS−PAGE then probed with the Ku70 C-19 C-terminal antibody is shown in Figure 5C. A second doublet was readily observed at approximately 37 kDa (denoted with an asterisk) which again was dramatically reduced in intensity in reactions where Ku was bound to DNA. To ascertain the origin of the 37 kDa doublet, an additional 15% SDS−PAGE gel was run and probed with a different Ku70 antibody (N3H10) which recognizes amino acids 506–541 (Figures 3 and 5D). The single and double asterisks refer to the generation of doublet peptides cut from Ku under non-DNA-bound conditions at 37 and 25 kDa, respectively. Therefore, the 10 kDa band represents a partial product from the 37 kDa band and must contain amino acids comprising a sequence after amino acid 541, since the 25 kDa band is recognized only by the N3H10 antibody. Thus, the 10 kDa band must represent the extreme C-terminal portion of the Ku70 SAP domain, and a reduction of peptides is observed with DNA binding Ku.

To more accurately determine the identity of the 10 kDa peptide that comprises the extreme C-terminus of Ku70, we excised the 10 kDa band and performed an in-gel tryptic digestion followed by LC−MS/MS analysis which detected 13 different peptides corresponding to the Ku70 subunit shown in Table 2. The majority of the peptides (8 of 13) mapped to the C-terminal region of Ku70 covering amino acids 545–605 and is represented by peptides 6–13 in Table 2. The other peptides that were discovered mapped to five distinct regions of Ku70 and appeared only one time each in the MASCOT database search with the exception of peptide 1, which appeared twice. This more random appearance of peptides is likely due to carryover from previous

Table 2: MS/MS Analysis of the 10 kDa Peptide[a]

peptide	mass	Ku70 peptide	amino acids
1	1573.82	NIYVLQELDNPGAK	101–114
2	1701.88	VHFEESSKLEDLLR	231–244
3	1651.85	TFNTSTGGLLLPSDTK	302–317
4	692.38	YTPRR	400–404
5	1806.91	MPFTEKIMATPEQVGK	446–461
6	1311.64	HDNEGSGSKRPK	545–556
7	2418.15	HDNEGSGSKRPKVEYSEEELK	545–565
8	1506.78	RPKVEYSEEELK	554–565
9	1125.53	VEYSEEELK	557–565
10	1691.85	VEYSEEELKTHISK	557–570
11	936.55	AYGLKSGLK	587–595
12	1557.92	SGLKKQELLEALTK	592–605
13	1172.69	KQELLEALTK	596–605

[a] Protein gel bands from Figure 4A (lanes 3, 5, and 7) were excised and subjected to an in-gel tryptic digestion procedure. Gel pieces were also cut from the same position in lanes 4, 6, and 8. LC−MS/MS was performed separately on each sample, and the sum identity of each individual peptide detected from all lanes is presented. There were not any detectable levels of Ku-specific peptides from lanes 4, 6, and 8. In both the number of different peptides and the appearance of individual peptides from lanes 3, 5, and 7, the majority mapped to the C-terminus of the Ku70 subunit (amino acids 545−605). These peptides were generated only in the absence of a Ku−DNA complex, suggesting a local conformational change.

LC−MS/MS runs. The list of peptides in Table 2 represents the sum of all the peptides detected. From simple addition of amino acids 545–605 that can be detected in the C-terminal region, a fragment corresponding to 7.333 kDa is derived. Additional peptides could have been generated from trypsin cleavage both N- and C-terminally from amino acids 545–605 on Ku70. The last four amino acids, HFQD (606–609), of Ku70 cannot be detected by mass spectrometry as a peptide alone or as part of a larger peptide. Also, N-terminal of residue 545, the VTKRK sequence could also be cleaved at two sites to generate a di- and tripeptide. Therefore, the possibility that these peptides are cleaved into smaller products and are too small to be detected exists, but it is more likely that these peptides were not trapped on the C8 material and flowed through to the waste from the HPLC during the sample run of LC−MS/MS. Another peptide that could have been generated, ELVYPPDYNPEGK (amino acids 527–539), was also not detected. Even though these three peptides flank the Ku70 C-terminal peptides that comprised the 10 kDa band, they were not detectable. On the basis of the difference in precision between Tris−Tricine PAGE and tandem mass spectrometry, it is not surprising that a disconnect was observed in the molecular masses of the peptide between the two methods.

Western blots probed with antibodies against the Ku70 C-terminus revealed a robust difference in the generation of the 10 kDa band between free and DNA-bound Ku. The C-19 antibody recognizes the far C-terminus of Ku70 (Figure 3) and detected two bands that are more predominant in intensity when Ku is not bound to DNA yet are detectable with Ku−DNA complexes in Figure 5B. This doublet corresponds to molecular masses of approximately 7 and 10 kDa. This experiment also utilized amounts of trypsin and Ku protein larger than those used in Figure 5A. The antibody recognizes a doublet around the 10 kDa protein standard. While the doublet appears in lanes containing free and DNA-bound Ku, the intensity markedly increases with increasing amounts of trypsin, and this trend is duplicated on an SDS−PAGE gel probed with the same antibodies in Figure 5C. It should be noted that while we were not able to detect the Ku70 C-terminal peptide, ELVYPPDYNPEGK, from in-gel tryptic digestion of the 10 kDa band, the majority of this peptide represented a critical change in biotinylation in Table 1. Thus, the sum of these data indicate that the Ku70 C-terminal domain appears to reposition itself by scaffolding or form new secondary structural features when it contacts duplex DNA.

DISCUSSION

The Ku protein is a critical component of the NHEJ pathway and possesses a very interesting structure which facilitates its role in DNA binding. While no significant differences in the high-resolution X-ray structure are apparent between free Ku and DNA-bound Ku, the dynamic nature of DNA binding suggests the potential for Ku conformational changes to accompany DNA binding. Previously, work from our laboratory demonstrated a reversible redox-dependent change in Ku structure that accompanied an alteration in DNA binding (*17*). We demonstrated that Ku−DNA complexes are stabilized in the presence of reducing agents such that the kinetic off rate is drastically slower than when Ku is bound to DNA under oxidized conditions (*17*). In addition, we were able to map redox-sensitive tryptic sites to the bridge and pillar region on Ku70, suggesting a conformational change in the protein under reducing conditions. This study confirmed earlier analysis of the effect of redox on Ku (*23*). Ku structure has also been assessed as a function of IP6 binding where a decreased level of protease digestion was observed in the presence of IP6 (*24*). The authors hypothesized this was a result of a conformational change in Ku, though they could not rule out other possibilities. This same report assessed protease digestion in the presence and absence of DNA, with Ku bound to DNA resulting in a reduced level of protease cleavage. However, the authors used sheared calf thymus DNA as a substrate for Ku which has the potential of generating a heterogeneous population of Ku−DNA complexes which complicates the analysis. The alteration in protease sensitivity was not mapped to either subunit or any specific region of Ku. While the three-dimensional crystal structure gives us a well-defined model of how the Ku−DNA interaction occurs, a significant portion of both Ku70 and Ku80 was not present in both the free and DNA-bound Ku crystal structures. In addition, these are static structures which represent snapshots of what are likely to be dynamic complexes.

Low-resolution electron microscopy analysis of Ku−DNA complexes confirms DNA-dependent conformational changes in Ku structure (*25*). To obtain a clearer picture of the potential Ku conformational changes as a function of DNA binding, we employed high-resolution chemical modification analysis of a homogeneous Ku−DNA complex.

In this work, we utilized chemical modification of lysines combined with mass spectrometry to identify specific amino acids in Ku that display differential reactivity upon DNA binding. Differential reactivity can be attributed to an altered structure of the protein or accessibility of the region to the modification reagent. This methodology has successfully identified novel protein−nucleic acid contacts on a variety of other proteins, including HIV reverse transcriptase and RPA (*26, 27*). Our analysis revealed that K331 was not

modified in the presence of DNA, and this amino acid lies within α-helix 9 (between β-sheets M and N) in the pillar region. The decrease in reactivity is attributed to a steric block afforded by the DNA such that K331, while not making direct DNA contact in the crystal structure, has reduced accessibility. In addition, K265 of Ku80 was also not modified in the presence of DNA, again a change that is directly attributed to steric hindrance from the DNA. Perhaps more interestingly, we were able to identify changes in the biotinylation status of specific lysine residues on peptides which represent the Ku70 C-terminal SAP domain, which is known to contact DNA directly. This series of biotinylations was observed only in the absence of DNA in the C-terminus of the Ku70 subunit. Biotinylations on peptides represented by residues K539 and K582 were consistent on two different DNA substrates and in multiple experiments. Therefore, these differential biotinylation events were interpreted as potential changes in the scaffolding architecture of the Ku70 C-terminal SAP domain.

Confirming this analysis, we observed a 10 kDa proteolytic fragment that was not observed in the presence of DNA, and this peptide mapped to Ku70 residues 545–605, again suggesting a change in the C-terminus of Ku70 from DNA-induced steric hindrance that altered protease accessibility. Amino acids 533–609 are not present in the Ku70 DNA-bound cocrystal. In addition, residues 538–559 are not observed in the non-DNA-bound structure. Interestingly, the 10 kDa proteolytic fragment mapped to amino acids 545–605, which represents a fair portion of the DNA-binding SAP domain of Ku70. Amino acids 538–559 that are missing from the crystal structure physically connect to a structure comprising three α-helices in the non-DNA-bound Ku structure within amino acids 560–609. This stretch of amino acids likely represents a movable hinge that twists into the major or minor groove of DNA and becomes partially blocked from trypsin digestion in the DNA-bound form. This observation is supported by the experiments with limited proteolysis and Western blotting with antibodies against the Ku70 C-terminal region. Digestion of this region occurs with generation of a 37 kDa peptide precursor labeled with one asterisk in Figure 5D with the next cut generating the 25 kDa band marked with two asterisks. The antibody (N3H10) used to probe this Western blot recognizes amino acids 506–541 of Ku70. The C-19 antibody recognizes the latter part of the C-terminus within the final 30 amino acids of Ku70 (Figure 3) and was used to probe the blots in panels B and C of Figure 5. The sequences that were identified in the 10 kDa peptide did not include amino acids 506–541 but followed that stretch of peptides. This explains why both Ku70 antibodies recognize the 37 kDa peptide cleavage product marked with one asterisk in panels B and C of Figure 5, yet only the C-19 antibody detects the 10 kDa peptide. These data suggest a direct interaction between the SAP domain and DNA. However, the tryptic digestion pattern and biotin modification patterns indicate changes in the unstructured region of Ku70 in amino acids N-terminal to the SAP domain. These results suggest the possibility that a SAP−DNA interaction is facilitated by the flexible linker region connecting the SAP domain to the base of the main DNA binding domain. Once again, the evidence points out that the C-terminal Ku70 SAP domain undergoes a change in secondary structural elements such that it scaffolds within the duplex DNA.

Given the importance of the Ku80 C-terminal domain in DNA−PKcs binding and the likelihood that binding of Ku to DNA manifests a structural change in this region, we sought to examine this possibility using the amino acid chemical modification assay. However, no detectable biotinylation differences were observed between the free and DNA-bound forms of Ku in the extreme Ku80 C-terminus. This is not entirely unexpected considering the structure of this region and the positioning of the lysines within this region. Two solution structures of the C-terminal region of Ku80 have modeled six α-helices binding with an extreme C-terminal unstructured loop dispensable for DNA−PKcs binding, while helices α2 and α4 have been described as being very hydrophobic and may represent binding pockets for protein–protein interactions (*13*). One could envision the flexible linker region of Ku80 driving large changes in the position of the C-terminus upon DNA binding without necessarily altering the accessibility of the lysine amino acids within helices α2 and α4. Consistent with this possibility was the demonstration that using limited proteolysis with site-specific antibodies we were able to detect conformational changes in this region of the Ku80 subunit. Generation of the higher-molecular mass doublet above the 19 kDa band in the absence of DNA represents the conformational change in Ku80 in Figure 4. This Ku80 DNA-dependent conformational change could cause this region to be more capable of accommodating DNA−PKcs binding for a stable interaction. The C-terminal region of Ku80 is critical for in vitro and in vivo activation of the DNA−PKcs complex (*28*). This region has been determined to directly interact with the DNA−PKcs complex, and removal of this region resulted in radiation sensitivity and impaired V(D)J recombination events (*15, 28*). Our data support and extend previous single-molecule structural EM analysis suggesting that the C-terminal domain of Ku80 undergoes limited movement upon DNA binding.

DNA-dependent steric hindrance changes in specific domains of Ku have direct implications for the DNA-dependent activation of the DNA−PK complex and involvement in other biological processes. Recently, the conserved α5 helix on Ku has been proposed to have an opposing role in telomere silencing on the Ku80 face and NHEJ on the Ku70 face in a yeast model system (*29*). Considering the essential role of the Ku80 C-terminus in DNA−PK activation, the question of how this interaction is influenced by DNA binding remains open. One can envision a change in the scaffolding of Ku70 and Ku80 CTDs upon DNA binding, thereby rendering these domains more accessible for docking the large 469 kDa DNA−PKcs component. In addition, disruption of this interaction may regulate post-kinase activities, including facilitating binding of other NHEJ components and release of Ku and the DNA−PKcs complex from the termini prior to ligation. Clearly, additional analysis of the role of DNA-dependent conformational changes and determination of the sites of DNA–protein contacts within the DNA−PK complex are required for elucidation of the complex mechanisms involved in DNA−PK activation.

ACKNOWLEDGMENT

We acknowledge members of the lab for critical reading of the manuscript. We also thank Drs. Randy Arnold and

Milos Novotny at Indiana University (Bloomington, IN) for their help with the MASCOT analysis.

REFERENCES

1. Burma, S., Chen, B. P., and Chen, D. J. (2006) Role of non-homologous end joining (NHEJ) in maintaining genomic integrity. *DNA Repair 5*, 1042–1048.
2. Baumann, P., and West, S. C. (1998) DNA end-joining catalyzed by human cell-free extracts. *Proc. Natl. Acad. Sci. U.S.A. 95*, 14066–14070.
3. McElhinny, S. A. N., Snowden, C. M., McCarville, J., and Ramsden, D. A. (2000) Ku recruits the XRCC4-ligase IV complex to DNA ends. *Mol. Cell. Biol. 20*, 2996–3003.
4. Niewolik, D., Pannicke, U., Lu, H., Ma, Y., Wang, L. C., Kulesza, P., Zandi, E., Lieber, M. R., and Schwarz, K. (2006) DNA-PKcs dependence of Artemis endonucleolytic activity, differences between hairpins and 5′ or 3′ overhangs. *J. Biol. Chem. 281*, 33900–33909.
5. Goodarzi, A. A., Yu, Y., Riballo, E., Douglas, P., Walker, S. A., Ye, R., Harer, C., Marchetti, C., Morrice, N., Jeggo, P. A., and Lees-Miller, S. P. (2006) DNA-PK autophosphorylation facilitates Artemis endonuclease activity. *EMBO J. 25*, 3880–3889.
6. McElhinny, S. A. N., Havener, J. M., Garcia-Diaz, M., Juarez, R., Bebenek, K., Kee, B. L., Blanco, L., Kunkel, T. A., and Ramsden, D. A. (2005) A gradient of template dependence defines distinct biological roles for family X polymerases in nonhomologous end joining. *Mol. Cell 19*, 357–366.
7. Ahnesorg, P., Smith, P., and Jackson, S. P. (2006) XLF Interacts with the XRCC4-DNA Ligase IV Complex to Promote DNA Nonhomologous End-Joining. *Cell 124*, 301–313.
8. Buck, D., Malivert, L., de Chasseval, R., Barraud, A., Fondaneche, M. C., Sanal, O., Plebani, A., Stephan, J. L., Hufnagel, M., le Deist, F., Fischer, A., Durandy, A., de Villartay, J. P., and Revy, P. (2006) Cernunnos, a novel nonhomologous end-joining factor, is mutated in human immunodeficiency with microcephaly. *Cell 124*, 287–299.
9. Gu, J., Lu, H., Tsai, A. G., Schwarz, K., and Lieber, M. R. (2007) Single-stranded DNA ligation and XLF-stimulated incompatible DNA end ligation by the XRCC4-DNA ligase IV complex: Influence of terminal DNA sequence. *Nucleic Acids Res. 35*, 5755–5762.
10. Yoo, S., Kimzey, A., and Dynan, W. S. (1999) Photocross-linking of an oriented DNA repair complex: Ku bound at a single DNA end. *J. Biol. Chem. 274*, 20034–20039.
11. Walker, J. R., Corpina, R. A., and Goldberg, J. (2001) Structure of the Ku heterodimer bound to DNA and its implications for double-strand break repair. *Nature 412*, 607–614.
12. Zhang, Z., Zhu, L., Lin, D., Chen, F., Chen, D. J., and Chen, Y. (2001) The three-dimensional structure of the C-terminal DNA-binding domain of human Ku70. *J. Biol. Chem. 276*, 38231–38236.
13. Harris, R., Esposito, D., Sankar, A., Maman, J. D., Hinks, J. A., Pearl, L. H., and Driscoll, P. C. (2004) The 3D solution structure of the C-terminal region of Ku86 (Ku86CTR). *J. Mol. Biol. 335*, 573–582.
14. Zhang, Z., Hu, W., Cano, L., Lee, T. D., Chen, D. J., and Chen, Y. (2004) Solution structure of the C-terminal domain of Ku80 suggests important sites for protein-protein interactions. *Structure 12*, 495–502.
15. Gell, D., and Jackson, S. P. (1999) Mapping of protein-protein interactions within the DNA-dependent protein kinase complex. *Nucleic Acids Res. 27*, 3494–3502.
16. Pawelczak, K. S., Andrews, B. J., and Turchi, J. J. (2005) Differential activation of DNA-PK based on DNA strand orientation and sequence bias. *Nucleic Acids Res. 33*, 152–161.
17. Andrews, B. J., Lehman, J. A., and Turchi, J. J. (2006) Kinetic analysis of the Ku-DNA binding activity reveals a redox-dependent alteration in protein structure that stimulates dissociation of the Ku-DNA complex. *J. Biol. Chem. 281*, 13596–13603.
18. Schagger, H., and Vonjagow, G. (1987) Tricine Sodium Dodecyl-Sulfate Polyacrylamide-Gel Electrophoresis for the Separation of Proteins in the Range from 1-kDa to 100-kDa. *Anal. Biochem. 166*, 368–379.
19. Gatlin, C. L., Kleemann, G. R., Hays, L. G., Link, A. J., and Yates, J. R. (1998) Protein identification at the low femtomole level from silver-stained gels using a new fritless electrospray interface for liquid chromatography-microspray and nanospray mass spectrometry. *Anal. Biochem. 263*, 93–101.
20. Turchi, J. J., Henkels, K. M., and Zhou, Y. (2000) Cisplatin-DNA adducts inhibit translocation of the Ku subunits of DNA-PK. *Nucleic Acids Res. 28*, 4634–4641.
21. Aravind, L., and Koonin, E. V. (2001) Prokaryotic homologs of the eukaryotic DNA-end-binding protein Ku, novel domains in the Ku protein and prediction of a prokaryotic double-strand break repair system. *Genome Res. 11*, 1365–1374.
22. Zhang, Z., Hu, W., Cano, L., Lee, T. D., Chen, D. J., and Chen, Y. (2004) Solution structure of the C-terminal domain of Ku80 suggests important sites for protein-protein interactions. *Structure 12*, 495–502.
23. Zhang, W. W., and Yaneva, M. (1993) Reduced sulphydryl groups are required for DNA binding of Ku protein. *Biochem. J. 293*, 769–774.
24. Hanakahi, L. A., and West, S. C. (2002) Specific interaction of IP6 with human Ku70/80, the DNA-binding subunit of DNA-PK. *EMBO J. 21*, 2038–2044.
25. Rivera-Calzada, A., Spagnolo, L., Pearl, L. H., and Llorca, O. (2007) Structural model of full-length human Ku70-Ku80 heterodimer and its recognition of DNA and DNA-PKcs. *EMBO Rep. 8*, 56–62.
26. Kvaratskhelia, M., Miller, J. T., Budihas, S. R., Pannell, L. K., and Le Grice, S. F. (2002) Identification of specific HIV-1 reverse transcriptase contacts to the viral RNA:tRNA complex by mass spectrometry and a primary amine selective reagent. *Proc. Natl. Acad. Sci. U.S.A. 99*, 15988–15993.
27. Shell, S. M., Hess, S., Kvaratskhelia, M., and Zou, Y. (2005) Mass spectrometric identification of lysines involved in the interaction of human replication protein a with single-stranded DNA. *Biochemistry 44*, 971–978.
28. Singleton, B. K., Torres-Arzayus, M. I., Rottinghaus, S. T., Taccioli, G. E., and Jeggo, P. A. (1999) The C terminus of Ku80 activates the DNA-dependent protein kinase catalytic subunit. *Mol. Cell. Biol. 19*, 3267–3277.
29. Ribes-Zamora, A., Mihalek, I., Lichtarge, O., and Bertuch, A. A. (2007) Distinct faces of the Ku heterodimer mediate DNA repair and telomeric functions. *Nat. Struct. Mol. Biol. 14*, 301–307.

BI702284C